Pathogenic Mechanisms in Ischemic Damage: A Computational Study

Eytan Ruppin and Elad Ofer
Depts. of Physiology and Computer Science
Tel-Aviv University, Tel-Aviv, 69978, Israel

James A. Reggia and Kenneth Revett and Sharon Goodall
Depts. of Neurology and Computer Science
University of Maryland, College Park, MD, 20742

July 29, 1997

Abstract

This paper presents a computational study of the pathogenesis of ischemic tissue damage during acute stroke. Two prime pathogenic mechanisms, cortical spreading depression (CSD) waves and glutamate excitotoxicity (GE), are investigated. Testable predictions describing the patterns of damage that arise if damage is caused by either mechanism are generated. These damaged tissue patterns are inherently different, arising from the distinct propagation characteristics underlying the CSD versus GE mechanisms. More specifically, when a V-shaped lesion is induced in a simulated area of decreased blood flow, the damage is almost circular in the CSD case, while in the GE case it follows more faithfully the shape of the initial lesion. When the center of the ischemic area is surrounded by ring-shaped lesion, tissue damage spreads outwards beyond the ring if the underlying mechanism is GE, but is completely blocked by the ring in the CSD case. The experimental testing of these predictions may help discriminate between the two pathological mechanisms postulated for ischemic tissue damage.

1 Introduction

Understanding the mechanisms underlying tissue damage in the ischemic penumbra is of paramount clinical importance: It may lead to new therapeutic measures that reduce evolving or progressing stroke, and the resulting post-infarct debilitation [1]. While considerable progress has been made in this area during recent years [2, 3, 4, 5], the mechanisms by which focal ischemia evolves into infarction and the factors which determine the ultimate extent of the infarct are still controversial [6, 7, 8, 9]. In this paper, we present a computational study of possible mechanisms that may underlie the spread of ischemic damage from the infarct core to the penumbra (peri-infarct) area. Our main interest is in the primary mechanisms that play a causal role in the activation of a cascade of metabolic events that eventually leads to penumbra tissue death. Towards this goal, we shall present a set of theoretical predictions that, if tested experimentally, may help in delineating the pathological mechanism(s) that play a primary role in this highly important pathological state.

There are two main hypotheses concerning the primary causal mechanism underlying penumbral tissue death during an acute ischemic stroke. The first theory is that ischemic (penumbral) damage is caused by the progression of *cortical spreading depression (CSD)* waves. CSD is a wave of reduced spontaneous electrical activity and biochemical changes that spreads across the cortex with a velocity of about $2-5$ mm/min. It is characterized by transient reductions in EEG power, failure of neurons to respond to evoked potentials, negative extracellular DC potential shifts, and increased extracellular potassium and L-glutamate [10]. Although occurring in the normally-perfused brain, CSD waves have also been found in ischemic tissue in various animal models of acute stroke, originating from the core of an infarct and progressing outwards into the penumbra (then also called ischemic depolarizations) [11, 12, 2, 3, 13, 9, 7]. The movement of CSD waves across the cortex may be viewed as a reaction-diffusion process involving potassium ions in the extracellular compartment [14, 15]. The reaction component increases extracellular K^+ levels by leakage from cells that have been necrotized or from intracellular K^+ released by the depolarization of cells. The released K^+ moves by diffusion out from the source in a radial fashion. Neurons and glial cells respond physiologically by increasing their Na/K-ATPase activity, which in turn reduces the levels of extracellular K^+. If the cells are compromised metabolically, this energy expenditure can deplete the energy reserves of the cells, generating a transient mismatch between energy supplies and demand, resulting in transient episodes of tissue hypoxia and lactic acidosis [16, 17, 13, 18]. The

ensuing gradual depletion of tissue ATP and high energy phosphate reserves following repetitive CSD waves may eventually lead to peri-infarct tissue death, depending on their frequency and duration [18].

The second hypothesis is that ischemic cell death is caused by neurotoxic mechanisms that occur *independently* of CSD waves. A variety of such mechanisms have been proposed, including the generation of oxygen free radicals and nitric oxide, and the recruitment of leukocytes and initiation of apoptosis [1]. The most prominent suggestion, however, has focused on the pathological role of *glutamate excitotoxicity (GE)*, which may occur independent of the existence of CSD waves. The main mechanisms that underlie high extracellular glutamate levels in the penumbra include depression of glutamate uptake processes due to energy deficiency, reversal of transport systems and cellular lysis (see [19] for a review). These mechanisms support the idea that glutamate neurotoxicity is a self-propagating process whose pathological effects are not curtailed by diffusional restrictions [20, 21]. In accordance with this concept, the increased glutamate levels originating from the dying tissue in the center of the infarct core spread outwards due to the action of a positive feedback process involving both glutamate diffusion in the extracellular space and ongoing tissue death. That is, the slow rate of glutamate diffusion outwards into the penumbra is markedly enhanced by the additional release of glutamate from cortical tissue damaged by glutamate excitotoxic effects. Moreover, the long range spread of of glutamate toxicity may be further enhanced by quasi-syncytial properties of the glial network, via which toxic metabolites can be transferred through tight junctions [22]. During middle cerebral artery occlusion the levels of extracellular glutamate in the penumbra may increase 25-fold, and the magnitude of glutamate release during ischemia is positively correlated with infarct volume [23]. A similar correlation between blood and CSF levels of glutamate and infarct size was recently observed clinically in human patients [24].

While both the CSD and glutamate excitotoxicity hypotheses involve self-propagating processes, they inherently differ in the nature of self-propagation. The CSD hypothesis assumes that tissue damage develops gradually due to the action of *repetitive*, relatively fast moving waves, that sweep across the penumbra a few times during the ischemic period. These repetitive waves have a common source, always originating at the rim of the infarct zone and progressing outwards in a concentric manner. In contrast, the GE hypothesis assumes that tissue damage develops due to the slow propagation of a single wave-front of glutamate. Unlike in the CSD case, where after the passage of a wave potassium levels may return to almost normal levels, in the GE case the levels of gluta-

mate in the regions traversed by the glutamate wavefront remain highly increased for a prolonged period of time. As we shall show, in appropriate situations these inherently distinct propagating characteristics can result in significantly different patterns of ischemic damage. [1]

Which of these two competing hypotheses is likely to be the primary causal factor responsible for ischemic penumbral damage? On the one hand, there is growing evidence that CSD waves do indeed play an important role in the pathogenesis of penumbra tissue damage. First, the number of waves traversing the penumbra has been found to strongly correlate with the extent of peri-infarct damage [3]. Second, recent diffusion-weighted magnetic resonance imaging studies have provided evidence that tissue damage propagation co-occurs with the passage of individual CSD waves [25]. Moreover, the CSD hypothesis seems to provide a better explanation than the GE hypothesis for the therapeutic effects of NMDA antagonists in focal ischemia [19]. On the other hand, however, there are several arguments that tend to favor the GE hypothesis over the CSD one. As noted by [26], the MRI findings of co-occurrence of tissue damage and CSD wave traversal may not reflect a real causal relationship between CSD waves and tissue damage, and may merely constitute an epiphenomenal manifestation of other underlying primary processes. That is, the CSD waves occur as an indicator of the ongoing rapid bursts of tissue damage, and not as their cause. In addition, there is evidence for hypoxic neural damage in the absence of CSD depolarizations in hippocampal slices [27]. Finally, unequivocal measurements of ischemic CSDs in humans are still lacking, although there is increasing evidence that CSD does occur in humans [28, 29]. Needless to say, it may also be the case that both mechanisms take part in causing ischemic damage. In the latter case, their respective relative importance should be determined.

In a previous paper we have studied in isolation the role of CSD waves in ischemic stroke, with the aid of a computational model [15]. We first verified the consistency of the model's behavior with normoxic and ischemic experimental data concerning the velocity, duration and general profile of CSD waves. We then systematically investigated how various physiological parameters interact and influence the ultimate amount of tissue damage for small, circular lesions. Following simulated infarction, our model displayed the linear relationship between final infarct size and the number of CSD waves traversing the penumbra that has been reported experimentally, even though dam-

[1] Glutamate has also been implicated in causing excitotoxic damage following the repeated occurrence of CSD waves. It should be re-emphasized that our study is not about whether glutamate plays a pathogenic role in penumbral tissue damage, but about the question of whether the underlying causal mechanism is best described by a repetitive wave process, or by the slow progression of a single wave front of damage.

age with each individual wave progresses non-linearly with time. It successfully reproduced the experimental dependency of final infarct size on mid-penumbra cerebral blood flow and potassium reuptake rates, and identified a critical penumbra blood flow rate beyond which damage does not occur. These results have provided support for the CSD hypothesis in stroke, and the model has generated testable predictions meriting further experimental investigation. The present paper relies on this basic CSD model (so that our previous findings remain valid now), but extends the model to include the description of GE processes, thus enabling us to address the causality issue directly, something that was not possible with our earlier version. Model extension is done in an incremental way, so that on all common variables the CSD and GE models' dynamical descriptions are identical. This approach provides a natural common scaling to both models, and assures their correspondence with our previous results.

2 Methods

The main problems one encounters when trying to study complex biological events like ischemic stroke is the richness of these phenomena and the incompleteness of relevant data. The large number of variables involved and their intricate and non-linear dependencies pose considerable difficulties. When constructing a formal model of such complex systems, these problems are further augmented by implementation issues. As a model becomes increasingly realistic, more computational resources are required, and the difficulty of visualizing the multi-dimensional information and interpreting the model's behavior increases dramatically. As a result, one needs to focus on a subset of key variables, and to determine convenient ways of tracing their temporal and spatial evolution. This approach was adopted by us in [15], and is followed here too. Below we provide a high-level overview of the mathematical model and its computational implementation. A more detailed technical description of the model is given in the Appendix.

In the model, the relations and interactions between the main variables of interest are expressed as a set of coupled differential equations. This formal model is implemented as a computer program, transforming the differential equations into a set of difference equations that are solved by numerical integration. Solving these equations numerically enables one to trace the model's evolution in time, given initial conditions and parameter settings.

2.1 The CSD Model

The model, first presented in [15], has been constructed according to two main guiding principles: to incorporate the presumed pathological role of CSD waves in the progression of peri-infarct damage, and to faithfully capture the basic characteristics of CSD waves in normoxic and ischemic tissue. The first guideline has determined the general structure of the model, i.e., its main variables and their mutual interactions; the model is specifically designed such that the propagation of CSD waves through penumbra tissue with impaired blood supply can cause an accumulative metabolic energy shortage, that may lead to progressive tissue damage. The second principle has mainly guided the choice of the model parameters, i.e., the strength of the interactions between the different model variables.

The model is based on a multi-dimensional set of non-linear differential equations that govern the temporal evolution of several key metabolic variables involved in CSD waves. Both the spatial structure of the cerebral cortex and time are discretized. The cortex is represented as a two-dimensional array of elements, each of which represents a small volume of cortex. One cortical element is 0.125 mm in length, and one time step corresponds to 13 msec [15]. Each cortical element i has its own value for extracellular potassium K_i, reuptake R_i, metabolic stores M_i, tissue intactness I_i, internal potassium stores S_i, and cerebral blood flow F_i. All variables incorporated into the model are dimensionless and are calculated and presented on a scaled basis from 0 to 1, as quantitative data on the rates of change for many of the variables in the model is unavailable.

The main ion involved in CSD waves is potassium. *The extracellular potassium* concentration (K_i) is modeled as a reaction-diffusion process governed by four terms: 1. A diffusion term which reflects the passive movement of potassium ions along their spatial concentration gradient. 2. A reaction term which models the regenerative processes that generates the CSD waves when K_i values exceed a threshold level. 3. A reuptake term which represents the reuptake of extracellular potassium by neuronal and glial Na/K-ATPase pumps; and 4. An infusion term reflecting intracellular potassium release to the extracellular space as a result of breakdown of neuronal membranes in dying ischemic tissue. *Potassium reuptake*, R_i, is proportional to the levels of extracellular potassium, tissue intactness and metabolic stores, and includes a decay term which brings Na/K-ATPase activity back to its resting level when K_i values are restored.

The levels of different metabolic factors that are important in defining the tissue energy state

(e.g., glucose and high energy phosphates) are combined together into a single variable M_i, the *metabolic stores level*. Their supply is proportional to the blood flow rate and tissue intactness, and their consumption is governed by the basal metabolic rate and reuptake demands. *Cerebral blood flow* (F_i) to a given cortical unit is modulated by that unit's metabolic stores and current level of cerebral blood flow. The magnitude of the hemodynamic response varies along the penumbra; cortical areas located closer to the infarct core receive further reduced blood supply and have a more significantly reduced hemodynamic response. *Tissue intactness* (I_i) denotes the fraction of cellular components that still remains viable. Tissue damage occurs in a cumulative fashion whenever the energy stores of a cortical element fall below a threshold value, and the extent of the damage is proportional to the extent and duration of the energy shortage. The tissue sensitivity to damage is modulated by the energy stress which the tissue undergoes, reflecting a growing susceptibility to damage of metabolically-comprised tissue. Finally, the rate of potassium effusion into the extracellular compartment is modulated by the level of *intracellular potassium stores*, S_i.

2.2 The GE Model

The basic structure of the model (and its computer implementation) is similar to the CSD model. As above, the model is based on a multi-dimensional set of non-linear differential equations that govern the temporal evolution of several key metabolic variables, this time those that are involved in GE. The cortex is represented as a discretized two-dimensional array of elements, each of which represents a small volume of cortex. The model's parameters are tuned such that the overall rate of damage progression into the penumbra is similar to that observed in the CSD case, so that its temporal and spatial scaling remain basically similar to that found in the CSD case. As in the CSD case, each cortical element i has its own value for reuptake R_i, metabolic stores M_i, tissue intactness I_i, and cerebral blood flow F_i. All variables are again dimensionless and are calculated and presented on a scaled basis from 0 to 1. The variables describing potassium dynamics in the CSD model (K_i and S_i) are replaced by variables describing the dynamics of glutamate and the corresponding excitotoxic damage. To model a self-propagating process involving a toxic metabolite, each cortical element i now has its own value of extracellular glutamate levels (G_i). As the cortical intactness level (I_i) decreases below a threshold level, glutamate is released from its intracellular stores (H_i). The rest of the variables and their dynamics remain identical to the CSD model described above.

The propagation of tissue damage in the GE model occurs as a result of leakage of glutamate

from dying, lesioned, tissue. Due to the impoverished energy stores and reduced glutamate uptake in the penumbra, elevated extracellular glutamate levels diffuse locally, causing further excitotoxic damage in adjacent tissue cells. Thus, an outward gradual spread of self-propagating excitotoxic tissue damage is induced. These processes are modeled in a straightforward manner (see Appendix). Extracellular glutamate levels G_i increase as a result of glutamate effusion from intracellular stores in damaged cortical tissue (the self-propagation term), and propagate through diffusion along the cortical grid. In turn, the rise of extracellular glutamate levels above a certain threshold level causes excitotoxic tissue damage. Finally, glutamate leakage out of damaged cells drains the intracellular stores (H_i), and ceases when these stores are completely depleted.

2.3 The Simulated Lesioning Experiments

To reiterate, the main goal of this work is to simulate cortical lesions with specific geometrical shapes in the center of the ischemic region, and to study the resulting patterns of penumbral tissue damage. To this end, in both the CSD and GE simulations, the cortical lesion is modeled by setting the tissue intactness at the center of the model cortex to zero (i.e., complete tissue death), according to the geometrical form of the simulated lesion (see Results Section). In addition, a penumbra gradient of cerebral blood flow is simulated. This gradient is modeled by linearly raising the blood flow from zero at the cortical elements in the center of the cortical grid to normal resting levels at the outermost elements of the penumbra. The radius of the penumbra in all the simulations is 35 cortical units.

Two kinds of lesions are simulated; V-shaped lesions whose vertex lies in the center of the cortex (see Figure 1), and ring-shaped lesions that surround the center of the penumbra at some distance from it. The length of each side of the V-lesion is 27 cortical units, and the width of each side is 10 units. The ring lesions were placed at distance of 20 units from the center of the penumbra, and their width was 4 units.

The simulations are stopped after damage has ceased to spread. This typically occurred after a computational time frame that is the equivalent of almost two hours in experimental animals.

2.4 Computer Implementation

The formal model described above and in detail in the Appendix has been implemented as a C program that runs under Unix. An Euler numerical integration method is used, and key results

have been verified using a fourth order Runge-Kutta method. In all simulations, the cerebral cortex is represented as a two dimensional sheet of cortical units (without modeling individual cellular components), each 0.125 mm wide, arranged in a hexagonal tessellation. The size of the two-dimensional array used in this paper is 100 x 100 elements ($\sim$ 1.2 cm per dimension).

To trace and visualize the behavior of the model, we generated two dimensional maps of the values of specific variables on the simulated cortex at a given moment. These maps can be displayed in a consecutive manner, providing an animated trace of the temporal evolution of these variables. In addition, some global quantities have been traced, such as the cumulative amount of tissue damage and the number of propagating CSD waves. The software required to run all of the simulations described in this paper, including the setting of all parameter values, is located at the *http://www.cs.umd.edu/~goodall/causality.html* website.

3 Results

Two scenarios are simulated. In the first, CSD waves are assumed to play the main pathogenic role; the dying tissue releases large amounts of potassium ions into the extracellular space, which in turn generate CSD waves that propagate outwards along the cortex, and cause further tissue damage. In the second, a GE diffusion-based self-propagating process is initiated, due to a large rise of extracellular glutamate that causes excitotoxic damage.

With many infarct lesions (e.g., roughly circular ones, like those observed in standard ischemic occlusion experiments), the resulting patterns of penumbra tissue damage are almost identical for both the GE and CSD cases. We therefore focused our research efforts on cortical lesions of two particular shapes that potentially promised to generate *distinct* patterns of damage, depending on the underlying pathogenic mechanism (CSD versus GE).

3.1 Differentiating CSD and GE Related Damage: A V-shaped Lesion

In the first experiment, we superimposed a V-shaped infarct lesion on the center of an ischemic region with reduced blood supply (see Figure 1). In the lesion region tissue intactness is clamped to zero to model cell death from mechanisms other than reduced blood supply (e.g., resulting from photo-infarction, or from topical application of toxic metabolites). The lesion is placed in the penumbra region such that the tip of the V-lesion lies in the center of the penumbra, which is also the center of each subfigure in Figures 1 and 3. The combined pathology of tissue death and

reduced blood supply (but not tissue death alone) results in a cascade of metabolic events that gradually causes damage to spread into the penumbra beyond its initial V-shaped borders.

The distinct patterns of tissue damage observed in these simulations following CSD or GE pathogenic mechanisms are shown in Figure 1. The damage in the GE case (e-h) follows the contours of the V lesion as it progresses. In the CSD case (a-d) the damage initially progresses more in the outward (left) region of the V lesion, but eventually it adopts an almost symmetrical shape around the center of the ischemic region. The parameters of the GE model are chosen such that the rate of damage progression in the GE case is of the same order as in the CSD case. In both cases, the rate of damage spread and its time course (a few *mm*s in about two-three hours) is in the same order of magnitude of that observed experimentally.

This computational experiment builds on the different generation and propagation characteristics of CSD versus GE mechanisms: CSD waves are generated when extracellular potassium levels increase above a threshold value. Since these levels are highest in the center of the penumbra (as reuptake is there the lowest), waves are first generated in this region, which hence becomes the driving, 'pace-maker' focus of the waves, as shown in Figure 2(a-d). The damage is caused in an accumulative manner, only after a few waves traverse the damaged region. These factors result in the formation of a fairly symmetric, circular propagating front around the lesion. GE spread, in contrast, depends on the propagation of a single glutamate wave front, that is generated simultaneously all along the lesion borders, and hence more faithfully preserves the shape of the initial lesion (e-h).

3.2 Blocking Tissue Damage Spread: A Ring-shaped Lesion

In the second experiment, we cut off the blood supply to the center of the simulated cortex, and impose a centrally-symmetric gradient of penumbral blood supply. We then simulate a ring-like lesion of dead cortical tissue by clamping the tissue intactness to zero in the ring lesion surrounding the ischemic core. As shown in Figure 3, while the damage spreads beyond the ring lesion in the GE case, its outwards spread into the cortical tissue is completely blocked if CSD waves are the dominant pathogenic mechanism.

This result shows that the propagation of CSD waves (and the accompanying damage) is more sensitive to dying tissue barriers than the spread of GE-related damage. The critical difference in the dynamics of CSD versus GE mechanisms underlying this phenomenon is that CSD propagation

heavily depends on the existence of *viable* cortical tissue; only viable tissue is capable of generating the 'reactivation' positive feedback loop required for the sharp rise of extracellular potassium that generates the CSD wave. In contrast, GE propagation arises mainly from the the leakage of glutamate to the extracellular space from the *dying* lesion area, that initiates a self-propagating loop of glutamate diffusion and tissue damage. That is, in contrast to CSD propagation, GE spread, is essentially independent of tissue intactness, and can more readily traverse damaged tissue regions.

The different propagation profiles of potassium and glutamate underlying the damage profiles depicted in the previous Figure, i.e., following a ring lesion placed in the penumbra, can be observed in Figure 4. The first CSD wave is initially generated at the site of the ring-shaped lesion, from where it spreads both inwards and outwards (see Figure 4a). However, this isolated CSD wave is not followed by any other CSD waves that originate from the ring lesion since potassium leakage from the damaged ring tissue dies out fairly quickly. Subsequent CSD waves emerge from the central core of dying ischemic tissue (c), but their propagation is blocked by the external ring lesion (b and d). In contrast, in the GE case (Figure 4, e-h), the damage is due to the gradual propagation of glutamate from dying cortical tissue in both the ring lesion and the infarct growing at the center of the penumbra. The ring lesion plays a dominant role in determining the resulting tissue damage, which spreads both inwards and outwards of the ring. [2]

To study the possible therapeutic implications of these findings, we tested the possibility of blocking the spread of CSD waves (and the corresponding damage) by generating a *functional* ring-shaped lesion surrounding the infarct core. That is, instead of having a ring of dead tissue, we altered parameters that characterize the functional status of the tissue *in the ring region only*, while keeping the cortical tissue in the ring region undamaged. We focused on two parameters that were found to play a key role in the propagation of CSD waves [15]: the parameter governing the rate of potassium "reaction" (c_{KA}, see Appendix), and the parameter governing the rate of potassium reuptake (c_{KK}). We find that the propagation of CSD waves beyond the functionally impaired ring area may be successfully blocked as long as the parameters mentioned above are kept below 30% of their original values. In contrast, we find that in the GE model the damage progresses beyond the ring lesion even if its width is significantly increased (to 10 units). Our simulations

[2]Note that the slow release rate of glutamate from the dying tissue compared with that of potassium is not a superfluous result of an arbitrary parameter setting. It arises from a fundamental constraint on the model construction; obtaining similar extent of damage spread into the penumbra after equal infarct time periods (or, alternatively viewed, reflecting the much slower propagation velocity of glutamate versus CSD waves).

show that the dysfunctional ring effectively blocks CSD propagation even if it is very close to the infarct core itself. However, we find that to effectively prevent the spread of damage, the ring region must be almost completely intact. That is, any gaps in the ring's continuity sharply decrease its protective potential. The resulting patterns of tissue damage with a functional ring-shaped lesion are essentially similar to those shown in Figure 3.

4 Discussion

The computational study presented in this paper has yielded two sets of predictions whose experimental testing may help delineate the prime pathological mechanism underlying penumbra tissue damage progression.

- We have examined the patterns of tissue damage that ensue when a V-shaped lesion is induced in a region of restricted blood supply. The resulting patterns are qualitatively different depending on whether the underlying pathogenic mechanism is CSD or GE dependent. In the CSD case, the patterns are essentially radially symmetrical, while in the GE case they preserve the V-shape of the original lesion. This difference is a fundamental one, arising from their distinct propagation characteristics.

- When the center of the penumbra region is surrounded by a ring-like lesion of dead tissue we find that, again, there is an inherent difference between the two mechanisms: CSD waves cannot pass such a barrier, while tissue damage caused by a GE mechanism does propagate outwards beyond the ring lesion. This difference is a robust and fundamental finding; GE-related damage continues to spread beyond the ring lesion even if the latter's width is significantly increased. Moreover, CSD waves do not propagate beyond the ring region even if it is not composed of dead tissue, but is only functionally compromised by reducing potassium reuptake or the potassium "reaction" feedback loop resulting in its sharp rise at the CSD wave front.

We find that the propagation of CSD waves can be blocked not only by inducing a 'protective' ring-like infarct, but also by altering the functional integrity of the tissue. The reduction of potassium reuptake models in a simplified manner the possible effects of partial blockade of Na/K pumps. Hence, perhaps surprisingly, our results suggest that the targeted delivery of ATPase blockers into a circumferential area surrounding the infarct core may help restrict the potential spread

of tissue damage. The reduction of the "reaction" term in the model has a less straightforward interpretation. It reflects a reduction in the magnitude of the positive feedback loop between membrane depolarization and potassium effusion that underlies the sharp rise of extracellular potassium during the passage of the CSD wave. Hence, therapeutic measures aimed at decreasing the conductance of voltage-dependent potassium channels, or at blocking calcium channels, may have promise in decreasing penumbral damage. It is hoped that in the future means for selectively targeting the penumbra regions with such therapeutic measures may be developed, without using invasive procedures that may be extremely hazardous in patients after acute, focal, stroke.

While it is possible to think that one mechanism is the primary causal one, in reality, it may also be the case that both CSD and GE play a joint causal role in the pathogenesis of penumbra damage. How then can one decipher their relative importance? In this paper, we present the first attempt to harness computational modeling to help advance an answer to this quandary. Being limited to the "computational drawing board", this kind of investigation cannot provide a definitive answer on its own. However, future experimental feedback addressing the predictions put forward herewith may help clarify the pathogenic factors underlying ischemic damage. Such Experimental studies can describe the patterns of damage that are observed when lesioning experiments of the the kind studied here are actually carried out *in vivo*. Since it is likely that in reality both mechanisms act in concert, at least to some degree, it may well be that these patterns may differ from those predicted in this paper. In this case, one can then re-use the computational model and simulation tools described in this work (available via our website) to learn more about the relative weights of CSD and GE mechanisms. To this end, the two mechanisms simulated here can be combined together into a unified model. Rerunning the combined model and searching for the best fit with the experimentally observed data can reveal the correct weighting.

In summary, the causal role of CSD waves and glutamate excitotoxicity in ischemic damage is currently still an open and important question [30]. This paper makes explicit predictions about the patterns of ischemic damage following acute focal ischemic stroke. The experimental study of these predictions may be feasible in the future (e.g., by using photo-infarction techniques [31, 32]), and may provide a clue to answering this question, by revealing the dominant pathogenic mechanisms underlying penumbral tissue damage. In reality, of course, both CSD and GE mechanisms may play a pathogenic role. Observing the actual experimental patterns of damage and comparing them to the 'canonical set' produced here may tell us about the relative weights of each mechanism in

the pathogenesis of penumbra damage. While the exact patterns observed depend on the specific parameter values used and may differ in reality from those shown here, we believe that our results will remain basically valid, since they arise from inherent differences in the propagation properties of CSD versus GE mechanisms.

References

[1] M. Fisher and J.H. Garcia. Evolving stroke and the ischemic penumbra. *Neurology*, 47:884–888, 1996.

[2] T. Iijima, G. Meis, and K.A. Hossmann. Repeated negative deflections in rat cortex following middle cerebral artery occlusion are abolished by MK-801. effect on volume of ischemic injury. *Journal of Cerebral Blood Flow and Metabolism*, 12:727–733, 1992.

[3] G. Mies, T. Iijima, and K.A. Hossmann. Correlation between peri-infarct dc shifts and ischaemic neuronal damage in rat. *Neuroreport*, 4:709–711, 1993.

[4] D.W. Choi. Glutamate receptors and the induction of excitotoxic neuronal death. *Progress in Brain Research*, 100:47–51, 1994.

[5] M. Fisher and J. Garcia. Evolving stroke and the ischemic penumbra. *Neurology*, 47:884–888, October 1996.

[6] W. Pulsinelli. Pathophysiology of acute ischaemic stroke. *The Lancet*, 339:533–536, 1992.

[7] K.A. Hossman. Viability thresholds and the penumbra of focal ischemia. *Annals of Neurology*, 36:557–565, 1994a.

[8] K.A. Hossmann. Glutamate-mediated injury in focal cerebral ischemia: The excitotoxin hypothesis revised. *Brain Pathology*, 4:23–36, 1994b.

[9] W.D. Heiss and R. Graf. The ischemic penumbra. *Current Opinion in Neurology*, 7:11–19, 1994.

[10] M. Nedergaard and A.J. Hansen. Characterization of cortical depolarizations evoked in focal cerebral ischemia. *Journal of Cerebral Blood Flow and Metabolism*, 13:568–574, 1993.

[11] M. Nedergaard and J. Astrup. Infarct rim: effect of hyperglycemia on direct current potential and 2-deoxyglucose phosphorylation. *Journal of Cerebral Blood Flow and Metabolism*, 6:607–615, 1986.

[12] R. Gill, P. Andine, L. Hillered, L. Persson, and H. Hagberg. The effect of MK-801 on cortical spreading depression in the penumbral zone following focal ischemia in the rat. *Journal of Cerebral Blood Flow and Metabolism*, 12:371–379, 1992.

[13] T. Back, K. Kohno, and K.A. Hossmann. Cortical negative DC deflections following middle cerebral artery occlusion and kcl-induced spreading depression: Effect on blood flow, tissue oxygenation, and electroencephalogram. *Journal of Cerebral Blood Flow and Metabolism*, 14:12–19, 1994.

[14] M. Lauritzen. Pathophysiology of the migraine aura: The spreading depression theory. *Brain*, 117:199–210, 1994.

[15] K. Revett, E. Ruppin, S. Goodall, and J.A. Reggia. Spreading depression in focal ischemia: A computational study. 1997. Submitted to the Journal of Cerebral Blood Flow and Metabolism.

[16] A. Mayevsky, N. Zarchin, and C.M. Friedli. Factors affecting the oxygen balance in the awake cerebral cortex exposed to spreading depression. *Brain Research*, 236:93–105, 1982.

[17] A. Mayevsky and H.R. Weiss. Cerebral blood flow and oxygen consumption in cortical spreading depression. *Journal of Cerebral Blood Flow and Metabolism*, 11:829–836, 1991.

[18] M. Gyngell, T. Back, and M. Hoehn-Berlage. Transient cell depolarization after permanent middle cerebral occlusion: and observation by diffuse-weighted MRI and localized 1H-MRS. *Magnetic Resonance in Medicine*, 31:337–341, 1994.

[19] F. Wahl, T.P. Obrenovitch, A.M. Hardy, M. Plotkine, R. Boulu, and L. Symon. Extracellular glutamate during focal cerebral ischaemia in rats: time course and calcium dependency. *Journal of Neurochemestry*, 63:1003–1011, 1994.

[20] D.W. Choi. Glutamate neurotoxicity and diseases of the nervous system. *Neuron*, 1:623–634, 1988.

[21] G. Garthwaite, G.D. Williams, and J. Garthwaite. Glutamate toxicity: An experimental and theoretical analysis. *European Journal of Neuroscience*, 4:353–360, 1992.

[22] C. Largo, P. Cuevas, G.G. Somjen, R.M. del Rio, and O. Herreras. The effect of depressing glial function in rat brain in situ on ion homeostasis, synaptic transmission, and neuron survival. *Journal of Neuroscience*, 16(3):1219–1229, 1996.

[23] K. Takagi, M. D. Ginsberg, M.Y. Globus, W.D. Dietrich, E. Martinez, S.Kraydieh, and R. Busto. Changes in amino acid neurotransmitters and cerebral blood flow in the ischemic penumbral region following middle cerebral artery occlusion in the rat: correlation with histopathology. *Journal of Cerebral Blood Flow and Metabolism*, 13:575–585, 1993.

[24] J. Castillo, A. Davalos, J. Naveiro, and M. Noya. Neuroexcitatory amino acids and their relation to infarct size and neurological deficit in ischemic stroke. *Stroke*, 27(6):1060–65, 1996.

[25] K. Takano, L.L. Latour, J.E. Formato, R.A.D. Carano, K.G. Helmer, Y. Hasegawa, C. Sotak, and M. Fisher. The role of spreading depression in focal ischemia evaluated by diffusion mapping. *Annals of Neurology*, 39:308–318, 1996.

[26] W.J. Koroshetz. Imaging stroke in progress. *Annals of Neurology*, 39(3):283–284, 1996.

[27] Z.F. Chen, F. Schottler, L. Arlinghaus, N.F. Kassel, and K.S. Lee. Hypoxic neuronal damage in the absence of hypoxic depolarization in rat hippocampal slices: the role of glutamate receptors. *Brain Research*, 708:82–92, 1996.

[28] R.P. Woods, M. Iacoboni, and J.C. Mazziotta. Bilateral spreading cerebral hypoperfusion during spontaneous migraine headache. *New England Journal of Medicine*, 331:1689–1692, 1994.

[29] A. Mayevsky, A. Doron, T. Manor, S. Meilin, K. Salame, and G.E. Ouknine. Repetitive cortical spreading depression cycle development in the human brain: a multiparametric monitoring aproach. *Journal of Cerebral Blood Flow and Metabolism*, 15 (1):534, 1995.

[30] T.P. Obrenovitch and J. Urenak. Altered glutamatergic transmission in neurological disorders: From high extracellular glutamate to excessive synaptic efficacy. *Progress in Neurobiology*, 51:39–87, 1997.

[31] R. Domann, G. Hagemann, M. Kraemer, H.J. Fruend, and O.W. White. Electrophysiological changes in the surrounding brain tissue of photochemically induced cortical infarcts in the rat. *Neuroscience Letters*, 155:69–72, 1993.

[32] L. Montalbetti, A. Rozza, V. Rizzo, L. Favalli, C. Scavini, E. Lanza, F. Savoldi, G. Racagni, and R. Scelsi. Aminoacid recovery via microdialysis and photoinduced focal cerebral ischemia in brain cortex of rats. *Neuroscience Letters*, 192:153–156, 1995.

[33] B. Grafstein. Locus of propagation of spreading cortical depression. *Journal of Neurophysiology*, 19:308–315, 1956.

[34] B. Grafstein. Mechanism of spreading cortical depression. *Journal of Neurophysiology*, 19:154–171, 1956.

[35] J. Bures, O. Buresova, and J. Krivanek. *The Mechanism and Application of Leao's Spreading Depression of Electroencephalographic Activity*, chapter 1. Academic Press, Inc, 1974.

Appendix: Formal Model Description

In the following equations, variables are denoted by a single capital letter (e.g., K, R), constant parameters by subscripts to the variables' names (e.g., K_{rest}, M_θ), and multiplicative constants begin with a lower case "c" which is subscripted by two capital letters, both of which are usually names of variables. The first letter is the name of the variable whose equation contains this constant, and the second letter is usually the name of a variable that the constant modulates (e.g., c_{KS} is the constant associated with the effect on the external potassium K of the internal potassium stores S). Numerical values for all parameters used in the simulations presented in this paper are listed in Table 3 at the end of this appendix.

Both the spatial structure of the cerebral cortex and time are discretized. The cortex is represented as a two-dimensional array of elements, each of which represents a small volume of cortex. A hexagonal tessellation of the cortex is assumed, so each element has six immediately adjacent neighbor elements.

A1: The CSD Model

Each cortical element i has its own value for extracellular potassium K_i, reuptake R_i, metabolic stores M_i, persistent impairment P_i, intactness I_i, internal potassium stores S_i, and cerebral blood flow F_i, governed by the equations below.

The rate of change of extracellular potassium concentration $K_i(t)$ of element i at time t is governed by the reaction-diffusion equation

$$\frac{\partial K_i}{\partial t} = c_{KA}(K_i - K_{rest})(K_i - K_\theta)(K_i - K_{max})(K_i + 0.1)I_i + c_{KS}(S_i - I_i)(K_{max} - K_i) - c_{KK}K_iR_i + c_{KD}\nabla^2 K_i \quad (1)$$

where $c_{KA} < 0; K_{rest}, K_\theta, K_{max}, c_{KS}, c_{KD} > 0; K_{inf} \geq 0$ are constants. Initially, $K_i = K_{rest}$ for all elements. The first term, the reaction term, meets the following requirements: homeostatic maintenance of resting extracellular potassium level K_{rest} (approx. 3 mM in the cortex), a threshold $K_\theta > K_{rest}$ beyond which elevated K_i triggers explosive subsequent growth in K_i, and a ceiling $K_{max} > K_\theta$ above which K_i does not rise. As these dynamics require normal mechanisms operative in undamaged tissue, this term is multiplied by the level of cortical intactness, I_i. The second term represents the pathological leakage of intracellular potassium into the extracellular space in damaged, infarcted tissue. It is a function of the levels of intracellular potassium stores S_i, tissue intactness I_i, and extracellular potassium. The third term reflects reuptake of potassium. The fourth term represents diffusion of K^+ through the cortex, where c_{KD} is the potassium diffusion coefficient and ∇^2 is the Laplacian operator. In order to implement the discrete form of the Laplacian operator, we multiplied the extracellular K_i level for element i by the number of neighboring elements and subtracted from this value the sum of the extracellular K values of these neighbors.

The rate of potassium reuptake, R_i, reflecting the functioning of membrane bound Na/K pumps, is modeled by

$$\frac{dR_i}{dt} = c_{RK}(P_\theta - P_i)I_iM_i(K_i - K_{rest}) - c_{RR}(K_{max} - K_i + c_R)R_i \quad (2)$$

The first term reflects reuptake proportional to the levels of partial impairment, tissue intactness, and extracellular potassium and the second is a decay term, which contains extracellular potassium-dependent and independent components. The initial value of R_i is 0.

The metabolic stores that determine the energy status of the tissue, such as glucose, and the high energy phosphate pool, are grouped together in a single variable M_i, and are governed by

$$\frac{dM_i}{dt} = c_{MF}F_iI_i(P_\theta - P_i)(M_t - M_i) - (c_{MR}R_i + c_{MM})M_i \quad (3)$$

where $c_{MF}, M_t, c_{MR}, c_{MM} > 0$ are constants. M_t is the equilibrium level of metabolic stores. c_{MM} is the basal level of energy expenditure. Initially, M_i starts at M_{rest}. The first term in equation (3) is a supply term, proportional to blood flow and tissue intactness levels, and inversely related to metabolic stores production rate. P_i is the partial impairment of element i, and the addition of the factor $(P_\theta - P_i)$ to the supply term incorporates the reduced ability of an impaired element to extract metabolic building blocks from the blood. The second term represent the metabolic load imposed by potassium reuptake and the basic metabolic rate.

The partial impairment variable P_i represents stresses on element i that compromise its integrity, such as decreased pH, increase in intracellular Ca^{2+}, etc. When the metabolic stores M_i drop below the partial impairment threshold (M_Θ), the partial impairment for cortical element i increases in proportion to the magnitude of the difference between M_Θ and M_i.

$$\frac{dP_i}{dt} = c_{PP}(M_\Theta - M_i)I_i \tag{4}$$

where $c_{PP} > 0$ is a constant. P_i remains unchanged when $M_i > M_\Theta$, and the initial value for P_i is 0.

Penumbra cerebral blood flow is regulated by

$$\frac{dF_i}{dt} = c_{FM}(M_{rest} - M_i)(F_{max} - F_i)I_i + c_{FF}(F_{max}/2 - F_i) \tag{5}$$

where $c_{FM}, M_{rest}, F_{max}, c_{FF} > 0$ are constants and $c_{FM} > c_{FF}$. M_{rest} is the initial metabolic stores level, F_{max} is the absolute ceiling for the blood flow rate and $F_{max}/2$ is the equilibrium rate of blood flow in normal tissue. Initially, F_i is $F_{max}/2$. The first term in (5) represents the dependency of blood supply on the status of the metabolic stores and current blood flow levels. The second term self-regulates blood flow towards its basal rate.

Variable I_i is an indicator of the intactness of element i, identifying the fraction of the element that is undamaged. Damage, which is assumed irreversible, occurs only below a critical metabolic threshold level $M_i < (P_\theta + P_i)$, and is proportional to this energy deficiency,

$$\frac{dI_i}{dt} = c_{II}(M_i - (P_\theta + P_i))I_i \tag{6}$$

where $c_{II}, P_\theta > 0$ are constants. I_i remains unchanged when $M_i \geq (P_\theta + P_i)$, and initially, I_i is 1.0. This threshold for tissue intactness is directly dependent on the persistent impairment P_i.

The leakage of potassium from intracellular to the extracellular space occurs when the intactness for a given cortical element, I_i, begins to drop. This formulation is expressed in the following equation,

$$\frac{dS_i}{dt} = c_{SS}(I_i - S_i) \tag{7}$$

where $c_{SS} > 0$ is a constant. Initially, S_i starts at 1.0.

Boundary conditions are set along the edges of the simulated cortex. The results are similar with leakage and sealed-end boundary conditions. In both cases, when CSD waves reach the edge of the simulated cortex, they dissipate immediately. This is consistent with numerous reports [33, 34, 35] indicating that CSD waves do not propagate across sulci. Since we have not included sulci in the present version of the model, these boundary conditions provide a functional equivalence to sulci with respect to CSD wave propagation properties.

The real-world equivalence of the duration and velocity of CSD waves can be calculated in a straight forward manner [15], yielding 0.125 mm as the cell scale and 13 $msec$ ($2.167 * 10^{-4}$ min) as the tick scale, the program time-step.

A2: The GE Model

The basic structure of the model (and its computer implementation) is similar to the CSD model. The cortex is represented as a two-dimensional array of elements, and both the spatial structure of the cerebral cortex and time are discretized. Boundary conditions are set as before. To model a self-propagating process of a toxic metabolite, each cortical element i now has its own value of extracellular glutamate levels (G_i). As the cortical intactness level (I_i) decreases below a threshold level, glutamate is released from its intracellular stores (H_i). All equations are similar to the CSD case, except for three changes:

1. Equation (1) governing extracellular potassium levels is now replaced by an equation governing extracellular glutamate levels. Instead of this former reaction-diffusion equation describing potassium-carried CSD waves we now have the following self-propagation equation

$$\frac{\partial G_i}{\partial t} = c_{GS}(S_i - I_i)(G_{max} - G_i) + c_{GD}\nabla^2 G_i \tag{8}$$

Extracellular glutamate stores are hence composed of two terms. The first denotes the leakage of glutamate out of damaged tissue (the self-propagation term), and the second denotes glutamate diffusion.

2. Tissue damage is now caused not directly as a function of metabolic deficiency (previously described in Equation (6), but due to the rise of extracellular glutamate levels beyond an excitotoxicity threshold I_θ,

$$\frac{dI_i}{dt} = -c_{II}(G_i - I_\theta) \tag{9}$$

where $c_{II} > 0$ is a constant. In parallel to the CSD case, I_i remains unchanged when $G_i \leq I_\theta$, and initially, I_i is 1.0.

3. Finally, glutamate leakage out of damaged tissue cells drains the intracellular stores, in accordance with

$$\frac{dH_i}{dt} = c_{HH}(I_i - H_i) \tag{10}$$

where $c_{HH} > 0$ is a constant. Initially, H_i starts at 1.0.

A3: Parameter values for both CSD and GE models

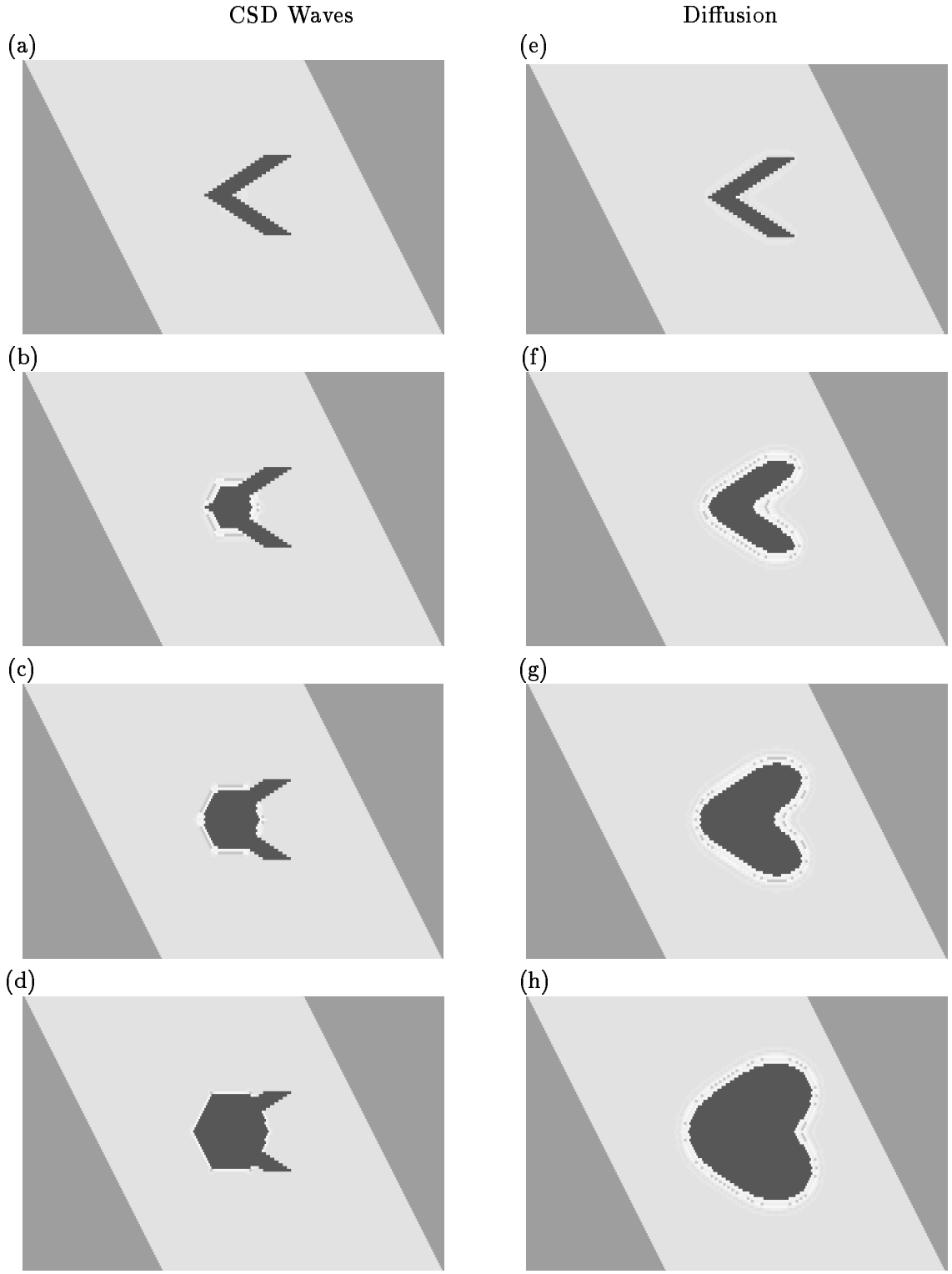

Figure 1: Propagation of penumbral tissue damage coupled with a V-shaped cortical lesion. The CSD case (a-d) is plotted in the left column, and GE case (e-h) in the right column. The four figures in each column show the level of damage at four 'snapshots'; initially, after 40 minutes of lesioning and reduced blood supply, after 80 minutes, and finally, after 2 hours, where the damage stabilizes and does not progress further. The figures' gray scale denotes tissue viability levels; white denotes completely viable tissue, while completely black color denotes dead cortical tissue. Each of the snapshot figures displays the whole simulated cortex (with a radius of 50 units), so that the simulated penumbra (with radius of 35 units) captures two-third of the distance outwards from the center of the display. This relation between the penumbra and simulated cortex dimensions holds

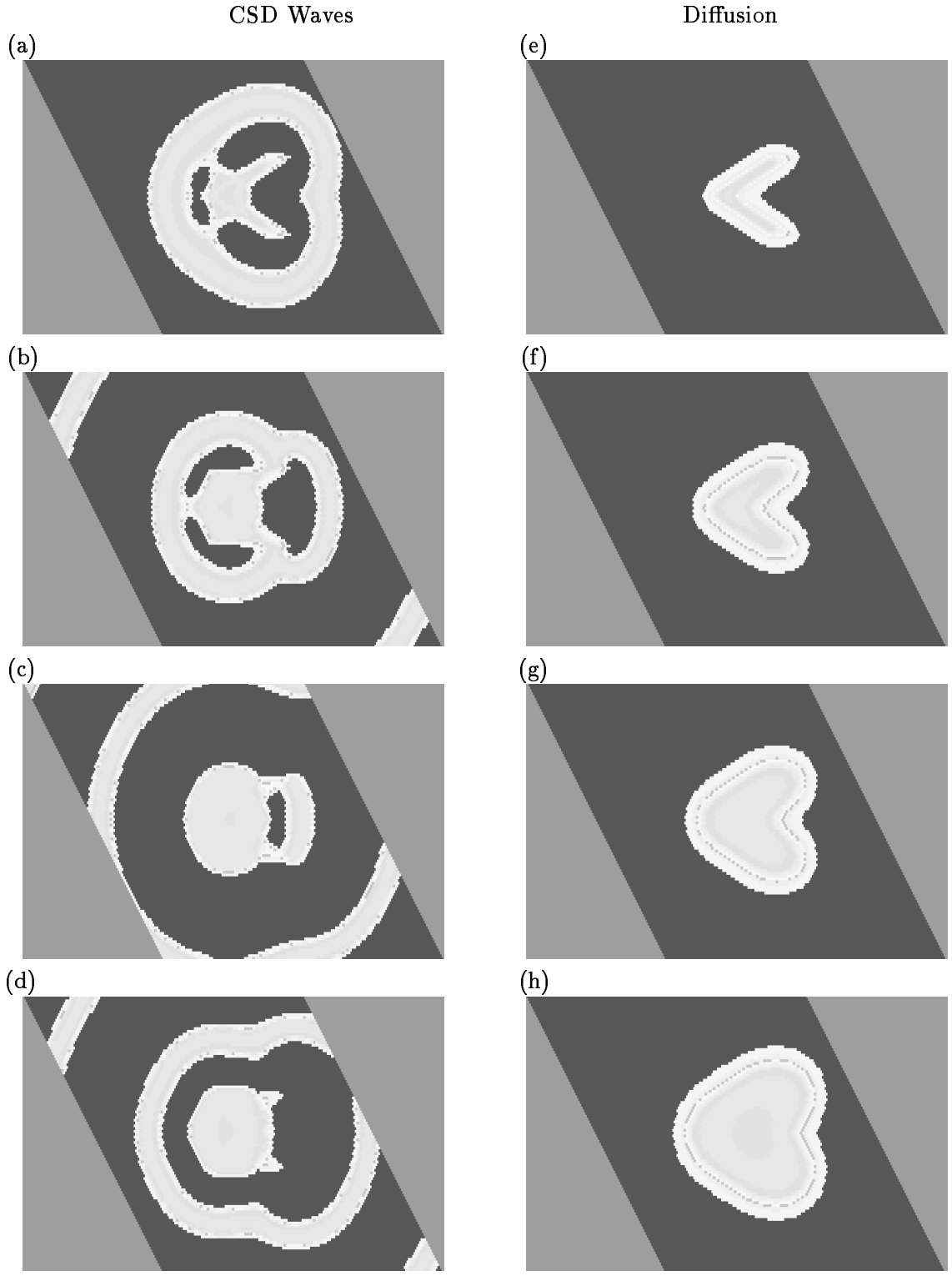

Figure 2: Propagation of potassium CSD waves (a-d) and glutamate (e-h) induced by a V-shaped cortical lesion. The four figures in each column show the levels of potassium and glutamate correspondingly in the simulated cortex at the same four 'snapshots' as in Figure 1. The white color now denotes regions of high levels of potassium (a-d) and glutamate (e-h). The propagation of a few CSD waves is depicted.

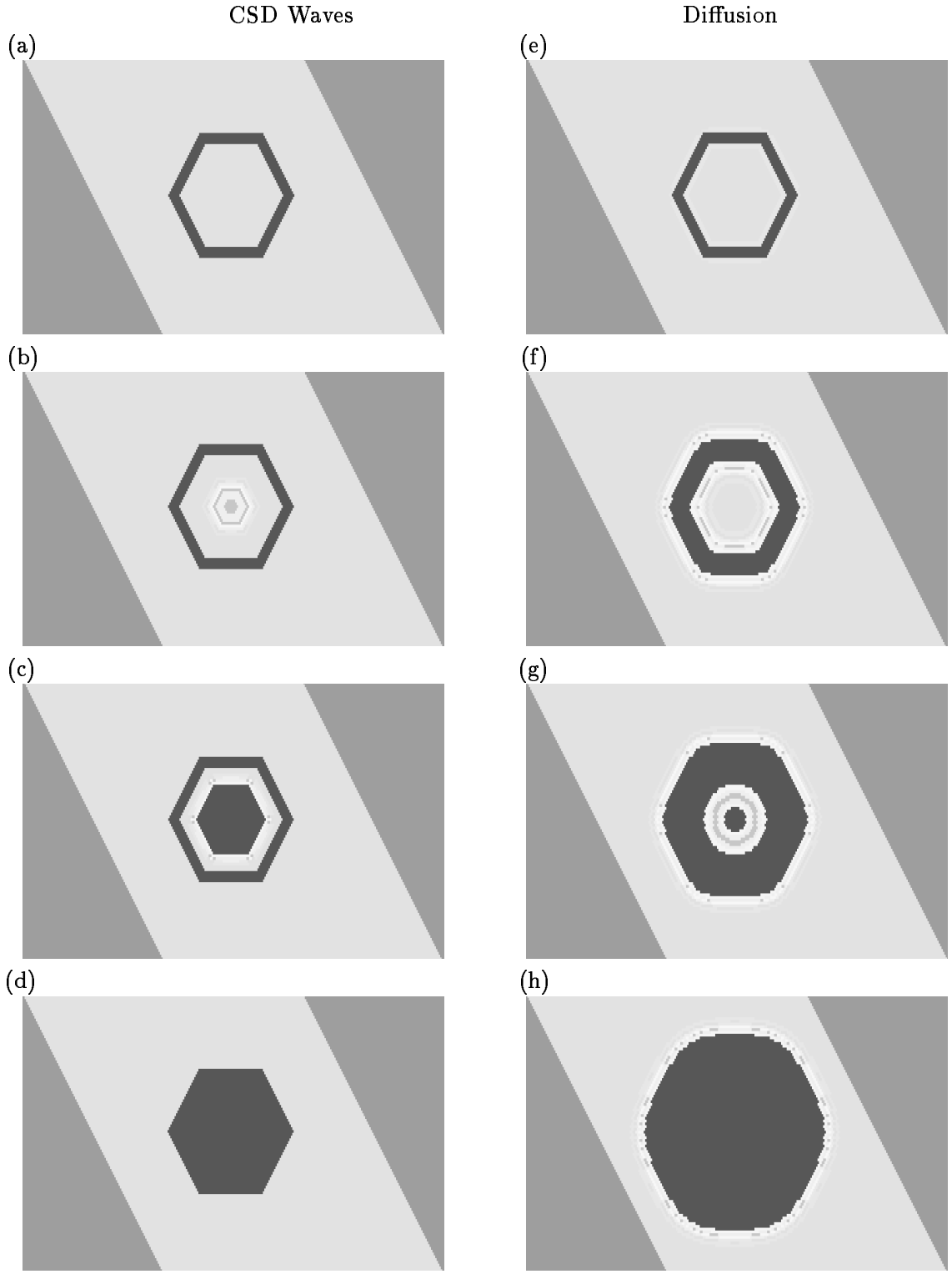

Figure 3: Blockade of the spread of penumbral tissue damage by a ring-shaped lesion. The CSD case (a-d) is plotted in the left column, and GE case (e-h) in the right column. As in Figure 1, the four figures in each column show the level of damage at four 'snapshots' at similar time intervals. Gray scale is similar to Figure 1.

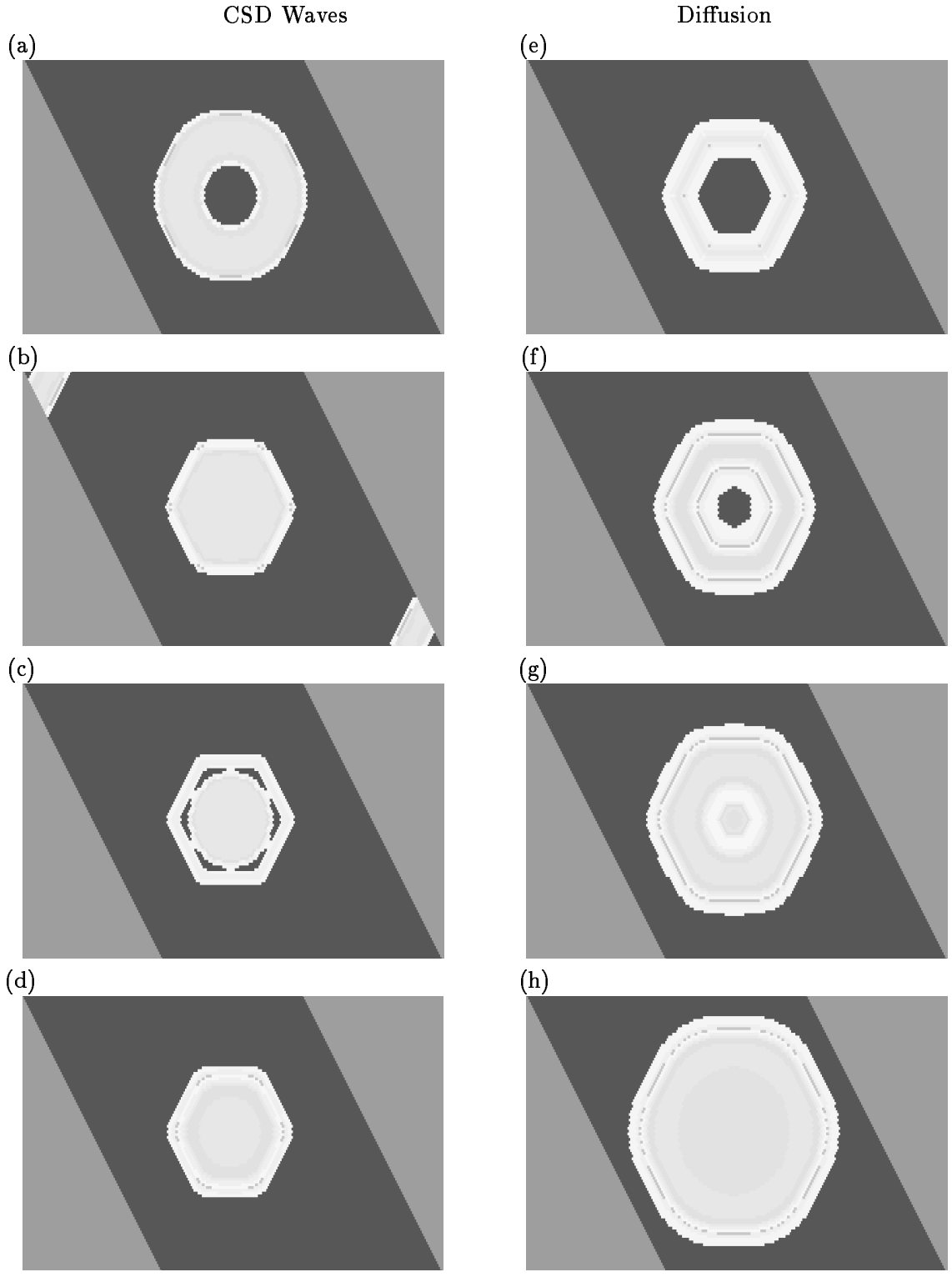

Figure 4: Propagation of potassium CSD waves (a-d) and glutamate (e-h) induced by a ring cortical lesion. Gray scale as in Figure 2. The four figures in each column show the levels of potassium and glutamate correspondingly in the simulated cortex at the same four time intervals. As evident, potassium spread is completely confined to the region inwards to the ring (except for the first CSD wave depicted in (a)). However, glutamate gradually spreads much beyond the region enclosed by the ring lesion (f-h).

Parameter	CSD Simulations	GE Simulations
K_{rest}	0.03	
K_{Θ}	0.20	
K_{max}	1.0	
c_{KD}	0.005	
c_{KS}	0.0035	
c_{KA}	-0.3	
R_{max}	1.00	1.0
c_{RR}	0.0006	0.0006
c_{RK}	0.00033	0.00033
M_{rest}	1.00	1.00
M_{Θ}	0.50	0.50
P_{Θ}	0.30	0.30
M_{max}	1.00	1.00
c_{MF}	0.0667	0.0667
c_{MM}	0.00025	0.00025
c_{MR}	0.30	0.30
M_t	$1 + 2M_{rest} * c_{MM}/c_{MF}$	$1+2M_{rest} * c_{MM}/c_{MF}$
c_{PP}	0.00015	0.00015
F_{max}	1.00	1.00
c_{FM}	5.00	5.00
c_{FF}	0.45	0.45
c_R	0.5	0.5
c_{SS}	0.0001	0.0001
K_i	0.03 (K_{rest})	
R_i	0.00	0.00
M_i	1.0 (M_{rest})	1.0 (M_{rest})
P_i	0.0	0.0
F_i	Graded[0–0.5]	Graded[0–0.5]
I_i	1.0	1.0
S_i	1.0	1.0
c_{II}	0.001	0.001
c_{GS}		0.0035
c_{GD}		0.005
G_{max}		1.0
I_{θ}		0.04
c_{HH}		0.0001